Published in final edited form as:

Cortex. 2016 March ; 76: 63–78. doi:10.1016/j.cortex.2015.11.020.

Resting-state low-frequency fluctuations reflect individual differences in spoken language learning

Zhizhou Deng[a,b], **Bharath Chandrasekaran**[c,d,e,f,g], **Suiping Wang**[a,**], and **Patrick C.M. Wong**[b,h,*]

[a] Center for the Study of Applied Psychology and Guangdong Key Laboratory of Mental Health and Cognitive Science, South China Normal University, Guangzhou, China

[b] Department of Linguistics and Modern Languages, The Chinese University of Hong Kong, Hong Kong

[c] Department of Communication Sciences and Disorders, Moody College of Communication, The University of Texas at Austin, Austin, TX, USA

[d] Department of Psychology, College of Liberal Arts, The University of Texas at Austin, Austin, TX, USA

[e] Department of Linguistics, College of Liberal Arts, The University of Texas at Austin, Austin, TX, USA

[f] Institute of Mental Health Research, College of Liberal Arts, The University of Texas at Austin, Austin, TX, USA

[g] Institute for Neuroscience, The University of Texas at Austin, Austin, TX, USA

[h] Brain and Mind Institute, The Chinese University of Hong Kong, Hong Kong

Abstract

A major challenge in language learning studies is to identify objective, pre-training predictors of success. Variation in the low-frequency fluctuations (LFFs) of spontaneous brain activity measured by resting-state functional magnetic resonance imaging (RS-fMRI) has been found to reflect individual differences in cognitive measures. In the present study, we aimed to investigate the extent to which initial spontaneous brain activity is related to individual differences in spoken language learning. We acquired RS-fMRI data and subsequently trained participants on a sound-to-word learning paradigm in which they learned to use foreign pitch patterns (from Mandarin Chinese) to signal word meaning. We performed amplitude of spontaneous low-frequency fluctuation (ALFF) analysis, graph theory-based analysis, and independent component analysis (ICA) to identify functional components of the LFFs in the resting-state. First, we examined the ALFF as a regional measure and showed that regional ALFFs in the left superior temporal gyrus were positively correlated with learning performance, whereas ALFFs in the default mode

[*]*Corresponding author*. G36, Leung Kau Kui Building, The Chinese University of Hong Kong, Shatin, New Territories, Hong Kong. p.wong@cuhk.edu.hk (P.C.M. Wong).. [**]*Corresponding author*. School of Psychology, South China Normal University, Guangzhou, 510631, China. wangsuiping@m.scnu.edu.cn (S. Wang).

Supplementary data

Supplementary data related to this article can be found at http://dx.doi.org/10.1016/j.cortex.2015.11.020.

network (DMN) regions were negatively correlated with learning performance. Furthermore, the graph theory-based analysis indicated that the degree and local efficiency of the left superior temporal gyrus were positively correlated with learning performance. Finally, the default mode network and several task-positive resting-state networks (RSNs) were identified via the ICA. The "competition" (i.e., negative correlation) between the DMN and the dorsal attention network was negatively correlated with learning performance. Our results demonstrate that a) spontaneous brain activity can predict future language learning outcome without prior hypotheses (e.g., selection of regions of interest – ROIs) and b) both regional dynamics and network-level interactions in the resting brain can account for individual differences in future spoken language learning success.

Keywords

Resting-state; fMRI; Low-frequency fluctuations; Spoken language learning; Individual differences

1. Introduction

Learning a new spoken language often requires learners to process novel speech categories and effectively use these new distinctions to distinguish word meaning. Spoken language learning outcomes vary greatly from learner to learner (e.g., Chandrasekaran, Sampath, & Wong, 2010; Chandrasekaran, Yi, Blanco, McGeary, & Maddox, 2015; Golestani & Zatorre, 2009; Wong, Perrachione, & Parrish, 2007). Individual differences often constrain learning success. Identifying critical individual differences in brain function that predisposes learners towards successful language learning is a dominant theme in recent spoken language learning studies (for review, see Zatorre, 2013). Methods that measure predisposing variables in these studies have included behavioral tasks, such as foreign sound contrast and discrimination tasks (e.g., Chandrasekaran et al., 2010; Golestani & Zatorre, 2009); cognitive tests, such as working memory and intelligence quotient (IQ) tests; genetic variation tests (Chandrasekaran et al., 2015; Wong, Chandrasekaran, & Zheng, 2012); and neuroimaging techniques, such as blood oxygen level-dependent (BOLD) activation within specific task designs (e.g., foreign vowel discrimination) using functional magnetic resonance imaging (fMRI) (e.g., Wong et al., 2007; Yi, Maddox, Mumford, & Chandrasekaran, 2014). These measures require participants to perform a specific task of varying complexity. However, numerous variations of these tasks limit the possibility of building a consistent framework of how individual differences contribute to spoken language learning. Thus, a measurement that is independent of task performance may be an ideal tool for studying spoken language learning.

Resting-state functional magnetic resonance imaging (RS-fMRI) is a neuroimaging method that focuses on spontaneous low-frequency (<.1 Hz) fluctuations (LFFs) in the BOLD signal (Biswal, Yetkin, Haughton, & Hyde, 1995; Fox & Raichle, 2007); the technique is gaining popularity as a means to measure intrinsic brain dynamics at rest without the constraint of task. RS-fMRI can be implemented in a data-driven manner. For example, spontaneous brain activity can be investigated independently of the regions of interest (ROIs) generated

in task-based fMRI studies (Wei et al., 2012). Additionally, individual differences in a large variety of cognitive task performances are reflected in spontaneous brain activity (Baldassarre et al., 2012; Supekar et al., 2013; Ventura-Campos et al., 2013). Harmelech and Malach (2013) proposed the spontaneous trait reactivation (STR) hypothesis to explain the consistent observation of an association between measures of spontaneous activity and cognitive task performance. According to the STR hypothesis, the LFFs reflect the profile of individual cortical biases. Thus, patterns in LFFs could provide a unique window for examining individual differences in cognitive traits and adaptive behavior. Taken together, RS-fMRI offers a promising and objective alternative for investigating predispositions in spoken language learning.

Recent studies have shown that spontaneous activity can be investigated via various approaches that provide complementary and converging evidence regarding the contribution of LFFs to various brain functions. Most studies have mainly focused on the properties of resting-state functional connectivity (RSFC), which reflects the strength of correlated intrinsic activity in distinct brain regions or ROIs (Friston, 2011). Because the selected ROIs are identified by task-related fMRI, analyses may be biased by task selection. In a study examining language learning, ROIs were identified by a phoneme identification fMRI task and used in conducting RSFC analyses (Ventura-Campos et al., 2013). Then, the RSFC was correlated with performance in another phoneme identification task that measured final learning outcome (Ventura-Campos et al., 2013). However, this study did not test the possibility of using RS-fMRI without the guidance of task-related fMRI or prior hypotheses to investigate individual differences in language learning. Here, we took advantage of the regional amplitudes of low-frequency fluctuations (ALFFs) as regional measures of spontaneous activity to explore the region-level contributions to learning in the resting-state. The advantages of ALFFs are that they are entirely data-driven and do not rely on a prior hypothesis. Recent studies have shown that ALFFs can reflect individual differences in performance in a large variety of cognitive tasks, including cognitive control (Mennes et al., 2011), object naming (Wei et al., 2012) and object color knowledge processing (Wang et al., 2013).

To examine the different aspects of intrinsic brain network dynamics, we applied two network analysis approaches, i.e., graph theory-based approaches and independent component analysis (ICA). Graph theory-based approaches describe the intrinsic brain network as a graph that consists of nodes and edges that provide statistical measures of the functional integration and segregation of all regions at the global level and specific regions within the entire brain network. The intrinsic brain network is topologically organized in non-trivial manners that include small-world networks and modularity (Bullmore & Sporns, 2009; J. Wang, Zuo, & He, 2010). In this study, graph-based nodal measures were applied to identify the role of a specific region of the whole brain network in learning; graph-based global measures were also applied to examine how the topological configurations of the whole brain are related to learning. While graph-based approaches utilize the brain as a large-scale network, ICA focuses on how the brain is organized into a number of discrete networks. The application of ICA has consistently identified two opposing systems, the default mode network (DMN) or “task-negative” network (Kelly, Uddin, Biswal, Castellanos, & Milham, 2008) and another system composed of “task-positive” resting-state

networks (RSNs), which include attention, visual, auditory, somato-sensory and language RSNs (Fornito, Harrison, Zalesky, & Simons, 2012; Smith et al., 2009). Similar to previous studies (Fornito et al., 2012; Kelly et al., 2008), network interactions between the DMN and the task-positive networks were evaluated. These interactions were used to investigate how inter-network dynamics contribute to learning. Using a combination of ALFFs, graph-based measures and ICA, we aimed to investigate how various aspects of spontaneous brain activity predict spoken language learning.

Learning a second language is a complex task in adulthood that requires considerable practice. Here, we focused on the ability to integrate novel complex sound patterns into lexical contexts. Sound-to-word learning emphasizes the ability to learn foreign sounds in the context of words. In this paradigm, native English-speaking participants were trained to associate pseudo-words that consisted of English pseudo-syllables and non-native pitch patterns with word meanings. For example, the syllable/pesh/was auditorily presented with a high level tone (Mandarin tone 1) whereas a picture of a glass was visually presented. The same syllable/pesh/with a rising tone (Mandarin tone 2) was associated with a picture of a pencil. To achieve successful learning, the participants had to use pitch patterns (tones) to signal word meanings (pictures). Our previous studies have shown that, after learning the contrasts of Mandarin tones in words during a training procedure over several days, native English participants learn to use these pattern changes to signal words to varying degrees (Chandrasekaran, Kraus, & Wong, 2012; Chandrasekaran et al., 2010; Wong, Chandrasekaran, Garibaldi, & Wong, 2011; Wong et al., 2007). More importantly, pitch patterns are typically not used to signal word meaning in English and some learners may have difficulty in learning (Wang, Spence, Jongman, & Sereno, 1999). Large individual differences have been consistently observed in previous studies using the sound-to-word paradigm. Given the large individual differences, we posit that sound-to-word training could be an ideal behavioral training procedure to investigate individual differences in spoken language learning. Regarding the neural substrates of sound-to-word learning, a left dorsal auditory stream has been proposed as a starting point for the phonological network according to duel-steam models (Hickok & Poeppel, 2007; Rauschecker & Scott, 2009); this stream has been shown to play an important role in sound-to-word learning in a traditional task-fMRI study (Wong et al., 2007). Furthermore, the topological configurations (e.g., graph theory-based measures) of task-related brain networks at both the regional and global levels are associated with speech comprehension (Sheppard, Wang, & Wong, 2011) and predict sound-to-word learning success (Sheppard, Wang, & Wong, 2012). These results suggest that variations in successful sound-to-word learning might be related to variations in brain dynamics at both the regional and network/global levels.

According to the STR hypothesis, individual differences in a priori cognitive biases (e.g., potential to master a new language) should be reflected in distinct spontaneous activity patterns, which can be measured by both regional spontaneous activity (i.e., ALFF) and correlation matrix among different cortical areas (i.e., graph theory-based measures and inter-network connectivity). We hypothesized that, the ALFF values and nodal measures from successful learning-related regions found in task-states, such as the left dorsal auditory regions, should positively correlate with learning performance. DMN not only plays a role in normal functioning (Whitfield-Gabrieli & Ford, 2012), but also involves in language

processing (Geranmayeh, Wise, Mehta, & Leech, 2014; Marcotte, Perlbarg, Marrelec, Benali, & Ansaldo, 2013). For example, more task-induced DMN deactivation was observed in the spoken language production task than in the simple counting task (Geranmayeh et al., 2014) and functional integration within the DMN predicted semantic feature analysis therapy in people with aphasia (Marcotte et al., 2013). We hypothesized that ALFF values and nodal measures from four core DMN regions, namely the medial prefrontal cortex (MPFC), posterior cingulate cortex (PCC), bilateral inferior parietal lobules (IPLs) and medial temporal lobe (MTL) should negatively correlate with learning performance. Furthermore, inter-network connectivity between DMN and task-positive network was found to be related to experience with using visual language (Malaia, Talavage, & Wilbur, 2014). We also hypothesized that, if the inter-network connectivity based on DMN plays a role in sound-to-word learning, the interactions between the DMN and task-positive RSNs should correlate with learning performance.

2. Materials and methods

2.1. Participants

Twenty right-handed adults (9 males; 25.90 ± 4.79 years old) participated in this study. The participants were native speakers of American English with no prior exposure to Mandarin Chinese or any other tone language (the language backgrounds were evaluated with the Language Experience and Proficiency Questionnaire, Marian, Blumenfeld, & Kaushanskaya, 2007). None of the participants were amateur or professional musicians, and had more than 6 years of continuous musical experience or learned music prior to 7 years of age. All participants passed a hearing screening test (<25 dB HL hearing thresholds at 500, 1000, 2000 and 4000 Hz). The participants provided informed consent in accordance with the Institutional Review Board of Northwestern University. Their nonverbal IQs (mean standard score = 119.35, SD = 11.17) were evaluated using the Test of Nonverbal Intelligence (Brown, Sherbenou, & Johnsen, 1997). The participants were also evaluated with two subtests from the Woodcock–Johnson Test of Cognitive Abilities (Woodcock, McGrew, & Mather, 2001): the Sound Blending (SB) test (mean percentile rank score = 80.10, SD = 16.71), which measures phonological awareness, and the Auditory Working Memory (AWM) test (mean percentile rank score = 85.72, SD = 10.70). Finally, individual differences in pitch pattern identification (mean proportion of correct tone identification = .84, SD = .14) were evaluated with a Tone Identification Test (Tone ID, Wong et al., 2007). Nineteen of these participants also participated in another structural MRI study, the results of which are not reported here (Wong et al., 2011). In this test, the auditory stimuli consisted of Mandarin vowels (/a/, /i/, /o/, /e/ and /y/) with Mandarin tones 1 (level), 2 (rising), 3 (dipping), and 4 (falling). The participants heard one stimulus and were required to press a button corresponding to the direction of pitch. The Tone ID score (the proportion of correct responses) was considered a behavioral measure of “nonlexical” pitch patterns prior to training because the participants were required to attend to the pitch patterns rather than the entire word. Previous studies have shown that Tone ID scores predict future sound-to-word learning success (Chandrasekaran et al., 2012; Wong & Perrachione, 2007). For further details about the stimuli and procedures of this test, see Chandrasekaran et al. (2012).

2.2. MRI scanning

For all participants, MR images were acquired using a Siemens 3T Trio MRI scanner (Erlangen, Germany). Axial anatomical images were acquired using a T1-weighted high-resolution 3D volume [MPRAGE; repetition time (TR) = 2300 msec, echo time (TE) = 3.36 msec, flip angle = 9°, matrix size = 256 × 256, field of view (FOV) = 22 cm, and slice thickness = 1 mm].

Functional images at rest were acquired axially using a susceptibility T2*-weighted echo planar imaging (EPI) pulse sequence (TE = 21 msec, TR = 2000 msec, flip angle = 90°, in-plane resolution = 3.4375 mm × 3.4375 mm, 36 slices with a slice thickness = 3 mm, and FOV = 220 mm). The participants were instructed to relax, close their eyes and remain awake throughout the 7-min scan (211 volumes).

2.3. Sound-to-word training procedure

The sound-to-word learning procedure used in the current study was identical to the procedures described by Chandrasekaran et al. (2010). Following the MRI scanning, the participants underwent a nine-day-training program in which they learned to associate monosyllabic pseudo-words with pictures. To learn the associations between the sounds and pictures, the participants had to become sensitive to changes in pitch patterns within each syllable. Six English monosyllabic pseudo-words (i.e., “pesh”, “dree”, “nuck”, “vece”, “fute”, and “ner”) were used to construct the stimuli. Using the Pitch Synchronous Overlap and Add (PSOLA) method provided by the Praat software (http://www.praat.org), each pseudo-word was superimposed with four pitch patterns that resembled the following Mandarin tones: 1 (level), 2 (rising), 3 (dipping), and 4 (falling). Thus, 24 words were constructed, and each word was paired with a picture that represented its meaning. To discourage rote memorization of the acoustic inputs and promote word learning (Lively, Logan, & Pisoni, 1993), a multi-talker approach (8 talkers) was used to construct the 24 words; thus, the stimuli from four talkers (2 males and 2 females) composed the training set materials, and the stimuli from the remaining talkers were used in the Generalization set.

There was no more than a 2-day gap between the training sessions. The 24 words were divided into six groups of four stimuli each. In the training session, the stimuli in each group were minimally contrasted in pitch, and were repeated four times per talker. To promote learning, the stimulus repetitions were blocked by the talker. At the end of each group, a test was conducted, and the participants were quizzed regarding the words they had just learned. The participants heard one of the four words and selected the correct image from the images they had just learned. During the quiz, feedback (correct/incorrect) was used to allow the participants to recognize and correct their mistakes. At the end of each training session, a final Word Identification Test was conducted. In this test, the 24 trained words were randomly presented to the participants, and they were asked to identify each word by selecting the corresponding images from 24 possible choices. This procedure was repeated for each talker. No feedback was given during the Generalization Test. The participants were provided with as much time as needed to identify the words. Each session, which included the training, practice quizzes, and the Generalization Test, lasted approximately 30 min. After the Word Identification Test in the final training session, the Generalization Test,

which included test items from the Generalization set, was administered according to the same procedure used in the Word Identification Test. The Generalization set was implemented to test how well the participants had learned the associations between the word sounds and meanings. All items in the Generalization set were words spoken new talkers. Thus, we were able to examine whether our participants recognized the words that they had learned in a new context (i.e., words spoken by new talkers). The Generalization Test score (correct proportion) was used as the final learning outcome in the present study. For the overall training procedure, please see Supplementary data.

2.4. Data analysis

2.4.1. fMRI preprocessing—RS-fMRI data were analyzed using the Statistical Parametric Mapping software (SPM8; http://www.fil.ion.ucl.ac.uk/spm), REST (Song et al., 2011) and the Data Processing Assistant for Resting-State fMRI (Chao-Gan & Yu-Feng, 2010). The first 10 volumes of the images were removed. The remaining volumes were corrected for slice-timing and motion. No participant exhibited head motion that exceeded 2 mm in translation or more than 2.5° in angular rotation along any axis. Next, each participant's anatomical image was co-registered to the mean functional image obtained from the slice correction and segmented into gray, white, and cerebrospinal fluid (CSF) tissue compartments. Then, the functional images were spatially normalized onto the Montreal Neurological Institute space using the parameters obtained during segmentation and resampled in 3-mm^3 voxels. The functional data were spatially smoothed with a 4-mm full-width at half-maximum (FWHM) Gaussian kernel. After removing the linear trend, a band-pass filter (.01–.08 Hz) was applied to retain the low-frequency signals.

Because ALFF is sensitive to signal in gray matter (Zang et al., 2007), a gray matter mask was generated by including the voxels with probabilities above .45 in the gray matter mask obtained by SPM8 and excluding the cerebellar regions (#91–#116) in the Automated Anatomical Labeling template (AAL, Tzourio-Mazoyer et al., 2002). Overall, there were 33061 voxels (892647 mm^3) in this gray matter mask. Further analyses were performed with this mask.

2.4.2. Regional analysis: ALFF calculation—The ALFF is defined as the total power in the low-frequency range (<.1 Hz), and it is equivalent to the standard deviation within a specific low-frequency band. To calculate the ALFF, time series were transformed to the frequency domain to obtain power spectra. The sum of amplitudes within the low-frequency range (.01–.08 Hz) was computed for each voxel. The square root was calculated at each power spectrum frequency. Each voxel's ALFF was taken as the average square root across .01–.08 Hz and was divided by the mean ALFF value within the gray matter mask to obtain a standardized value (Zang et al., 2007).

Correlation results indicated that both Tone ID scores and IQs before training were significantly correlated with Generalization scores (for details, see the Results). To evaluate the unique contribution of intrinsic brain activity to Generalization, partial correlations between Generalization scores and each voxel's ALFF value across the whole brain were performed, while controlling for the effects of pre-training Tone ID and IQ. The effects of

Tone ID and IQ were also controlled in all of the brain-behavior partial correlations that were performed as described below. For the ALFF-behavior correlations, the corrected threshold was set to a single voxel $p < .05$ with a cluster size > 54 voxels (1458 mm^3). The threshold was determined based on a Monte Carlo simulation that was implemented by the AlphaSim program in REST. Partial correlations between the mean ALFF value in each significant region and Generalization scores were also calculated while controlling for the effects of pre-training Tone ID and IQ (for anatomical regions and abbreviations, see Table 1).

2.4.3. Graph theory-based measures—The graph theory analyses were based on the data that were preprocessed as previously described without spatial smoothing to avoid local correlation artifacts (Sanz-Arigita et al., 2010). Additionally, the six head-motion parameters, the CSF and the white matter signals were removed by multiple linear regression. We did not regress out the global mean signal to avoid negative correlations (Rubinov & Sporns, 2010). Similar processing with the global mean signal regression was conducted, and the results were minimally altered. Please see Supplementary data. The Brain Connectivity Toolbox (BCT, http://www.brain-connectivity-toolbox.net/) was used for graph analysis.

The network nodes were defined by segmenting the data into 90 regions (45 regions per hemisphere) using the AAL template (Tzourio-Mazoyer et al., 2002). For each participant, the time series of each region was extracted by averaging the time series across all voxels in the region. Pearson's correlation coefficients between the time series of each possible pair of the 90 regions were subsequently calculated to generate a symmetric correlation matrix. Each correlation matrix was thresholded to obtain an undirected binarized graph in which nodes represented regions and the edges represented connections. A fixed network cost value (defined as the total number of edges in a network divided by the maximum possible number of edges) was used to threshold each correlation matrix. This approach ensured that each network had the same number of edges or wiring cost. For a binary graph G_w with N nodes, the edge between the nodes (*I*,*j*) is represented by a_{ij}, which is either 1 if an edge exists between these two nodes ($a_{ij} = 1$ if $|r_{ij}|$ r_c, where r_{ij} represents the correlation between nodes *i* and *j* and r_c represents the cost threshold), or 0 if it does not ($|r_{ij}| < r_c$). To ensure that the results were not dependent on a specific cost value, each correlation matrix was thresholded over a range of .10–.40 at intervals of .02. The parcellation scheme of the AAL-1024 atlas (512 ROIs for each hemisphere) was based on the method reported in previous studies (Fornito, Zalesky, & Bullmore, 2010; Zalesky et al., 2010).

2.4.3.1. Global efficiency of the whole network: The shortest weighted path length linking nodes *i* and *j* (L_{ij}) equals the lowest number of edges that connect node *i* to each other node *j*. The global network efficiency represents the overall capacity for parallel information transfer and integrated processing and is defined as follows (Latora & Marchiori, 2001):

$$E_{\text{global}} = \frac{1}{N(N-1)} \sum_{j \in a_{ij}} \sum_{i \in a_{ij}, j \neq 1} \frac{1}{L_{ij}}.$$

2.4.3.2. Local efficiency of the whole network: The local efficiency on node *i* (E_i) gauges the efficiency of information flow within the local subgraph G_i of the nodes that are directly connected to (but not including) node *i*. The local efficiency of node *i* is as follows (Latora & Marchiori, 2001):

$$E_i = \frac{1}{(K_i)(K_i - 1)} \sum_{j,k \in G_i, j \neq k} \frac{1}{L_{jk}}.$$

where K_i equals the number of nodes directly connected to node *i*.

The local efficiency of the whole network is calculated as the average of the efficiency E_i over all subgraphs included in the network (Latora & Marchiori, 2001).

$$E_{local} = \frac{1}{N} \sum_{i \in G_w} E_i.$$

2.4.3.3. Nodal degree (D_{NODAL}): For the local property on the node *i*, we defined subgraph G_i, which includes all of the directly connected neighboring nodes of the node *i*. The node degree is the number of links connected to the node. The degree of node *i* is as follows (Bullmore & Sporns, 2009):

$$d_i = \sum_{j \in G_i} a_{ij}.$$

2.4.3.4. Nodal efficiency (E_{NODAL}): The nodal efficiency was defined as the inverse of the harmonic mean of the minimum length of path between node *i* and all other nodes. It measures the ability of a node to exchange information with the other nodes in a network. The nodal efficiency of node *i* is defined as follows (Achard & Bullmore, 2007):

$$E_{nodal} = \frac{1}{N - 1} \sum_{i \neq j \in G} \frac{1}{L_{ij}}.$$

2.4.3.5. Nodal betweenness (N_{BC}): Nodal betweenness measures the centrality of node *i* in a whole network. It is defined as follows (Freeman, 1997):

$$N_{bc} = \sum_{i \neq j \in G} \frac{\delta_{jk}(i)}{\delta_{jk}}.$$

where δ_{jk} is the number of shortest paths from node j to node k, and $\delta_{jk}(i)$ is the number of shortest paths from node *j* to node *k* that go through node *i* within graph G_i.

For all the network measures, we computed summary measures by averaging the values across the entire network cost range (from .1 to .4). Finally, we performed partial

correlations between the network measures (global network measures: E_{global}, E_{local}; nodal measures: d_{nodal}, E_{nodal}, N_{bc}) and Generalization scores while controlling for the effects of Tone ID and IQ. A permutation test (5000 random permutations) was performed to determine the critical lower/upper correlation coefficients. When the threshold was not met, we used an arbitrary threshold of $p < .005$ when reporting the results.

2.4.4. ICA method—The ICA analyses were based on the preprocessed data. We performed spatial ICA using Group ICA from the fMRI Toolbox (http://mialab.mrn.org/software/gift/). The dimensionality of the data was reduced from 201 (number of time points) to 67 through a two-step principle components analysis (PCA) and data concatenation. The number of components was determined using the minimum description length (MDL) criterion (Rissanen, 1978). Group ICA was performed on the reduced data using the Informax algorithm provided by the software. The time courses and spatial maps of each component were back-reconstructed. Both the spatial maps and the time courses were scaled using Fisher's Z-scores. To identify the voxels that were significantly different from zero, one-sample t-tests were conducted with the subject-specific spatial maps. The corrected threshold was set at single voxel $p < .05$ with a cluster size >56 voxels (1512 mm^3). The threshold was determined based on a Monte Carlo simulation implemented by the AlphaSim program in REST.

According to previous literature (Mueller et al., 2013; Smith et al., 2009; Whitfield-Gabrieli & Ford, 2012), these spatial maps have been used to identify the following RSNs: the DMN, the cingulo-opercular network (CON), the dorsal attention network (DAN), the fronto-parietal network (FPN), the left language network (LLN), the right language network (RLN), the visual network (VN), the auditory network (AN), and the somato-motor network (SMN).

The network interaction analyses were based on the preprocessed data previously described using spatial smoothing. Additionally, the six head-motion parameters, the CSF and white matter signals, and the global mean signal were removed by multiple linear regression. For each participant, the time series of each of the identified RSN was extracted by averaging the time series across all voxels of the RSN.

Two methods were used to calculate the network interactions between the DMN, CON, DAN, FPN, LLN, RLN, VN and SMN. The first approach involved full correlation analyses between the DMN and each of the seven networks. The second approach involved partial correlation analyses between the DMN and each of the other networks while controlling for the effects of the remaining networks (Fornito et al., 2012). After transforming these r values into Fisher's Z-scores, a one-sample t-test was performed to examine whether the connectivity was different from zero. To evaluate the contribution of the network interactions to Generalization, the partial correlation between Generalization scores and the network interaction was calculated while controlling for the effects of Tone ID and IQ. Because the aim of the exploratory analysis was to show the overall correlation patterns, multiple comparison correction was not conducted.

3. Results

3.1. Sound-to-word learning performance

As shown in Fig. 1, the learning curves of the 20 participants indicated that the training procedures improved their performance to various degrees. A mean proportion of correct performance of .642 (SD = .235) was achieved in the Generalization Test and was above the .2 chance level [$t(19) = 8.43$, $p < .001$]. As shown in Table 2, both Tone ID scores and IQs were significantly correlated with Generalization scores. Because our main aim was to evaluate the unique contribution of intrinsic brain activity to final learning outcome, we controlled the effects of pre-training Tone ID and IQ when using LFF measures to predict Generalization.

3.2. Brain regions related to sound-to-word learning: ALFF analysis

To evaluate the unique contribution of regional spontaneous activity to sound-to-word learning, we partially correlated Generalization scores with the ALFF value of each voxel across the whole brain while controlling for the effects of Tone ID and IQ. As shown in Table 3 and Fig. 2, negative correlations between ALFF values and Generalization scores were observed. The LSTG was the only region in which ALFF values were positively correlated with Generalization scores. Negative correlations between ALFF values and Generalization scores were identified in the several clusters, including PCUN/PCG, RITG, ORBmid, RSFGdor, RACG/LSFGmed, RANG/RMTG, RIPL/LANG and RSFGmed.

3.3. Brain regions related to sound-to-word learning: graph theory-based approaches

The global network properties, including E_{global_90}, E_{local_90}, E_{global_1024}, and E_{local_1024} were not significantly correlated with generalization scores ($r = -.42$, $p = .085$, $r = -.45$, $p = .061$, $r = .19$, $p = .46$, $r = .33$, $p = .18$, respectively). For the nodal measures, most results did not meet the threshold estimated by permutation tests (the critical correlation coefficients were shown in Table 4). We reported the results with uncorrected $p < .005$. As shown in Table 4, Fig. 3 and Fig. 4, nodal measures in the following regions were correlated with Generalization scores: LSTG (AAL-90/AAL-1024) in nodal efficiency and nodal degree analyses, LANG (AAL-90), LPCG (AAL-90) and PCUN (AAL-1024) in nodal degree analysis. More importantly, both ALFFs and nodal measures in these regions were significantly correlated with Generalization scores.

3.4. Network analysis: group-level interactions between the DMN and other RSNs

Using ICA, the DMN, FPN, CON, DAN, AN, VN, and SMN were identified as single components, whereas the language network comprised two separate systems: a left language network (LLN) and a right language network (RLN, Fig. 5). Fisher's Z-scores for the full correlations between the DMN and each of the other RSNs (method 1) indicated that the DMN activity was anticorrelated with the FPN ($r = -.12$), CON ($r = -.29$), DAN ($r = -.58$), LLN ($r = -.22$), RLN ($r = -.42$), AN ($r = -.26$), VN ($r = -.10$), and SMN ($r = -.45$). With the exception of the DMN-VN pair value, all values were significantly different from zero. As shown in Table 5 and Fig. 6, partial correlations of these r values with Generalization scores (Tone ID and IQ were covariates), revealed that DMN-DAN values were correlated

with Generalization scores (r = .50, p = .035), DMN-VN values were marginally correlated with Generalization scores (r = .41, p = .098), and the other values exhibited no significant correlations.

Consistent with the full correlation (method 1) results, the partial correlations between the DMN and each of the other RSNs (method 2) indicated that the DMN activity was anti-correlated with the FPN (r = −.14), CON (r = −.29), DAN (r = −.57), LLN (r = −.23), RLN (r = −.42), AN (r = −.26), VN (r = −.12), and SMN (r = −.43). With the exception of the DMN-VN pair value, all other values were significantly different from zero. As shown in Table 5 and Fig. 6, DMN-DAN values were correlated with Generalization scores (r = .52, p = .026), DMN-VN values were marginally correlated with Generalization scores (r = .45, p = .06), and the other values exhibited no significant correlations.

4. Discussion

How to use various aspects of spontaneous LFFs to predict future spoken language learning success without prior hypotheses remains unexplored (Baldassarre et al., 2012; Supekar et al., 2013; Ventura-Campos et al., 2013). Here, we applied an ALFF method, graph-based nodal measures and ICA to provide converging evidence that the spontaneous activities of specific regions objectively predict learning success without reliance on a pre-training task that is closely related to the content the participants are require to learn. Previous RS-fMRI studies have reported correlations between cognitive task performance and ALFF or graph-based nodal measures (Mennes et al., 2011; Wang et al., 2013; Wei et al., 2012). However, to the best of our knowledge, the current study is the first to demonstrate that ALFFs and graph-based nodal measures are predictive of post-training learning success prior to training experience in a completely data-driven manner. Additionally, network interaction analyses revealed that anticorrelations between ICA-identified RSNs, such as the DMN and DAN, can be inter-network-level predictors of learning capacity. Traditional task-related fMRI studies of speech processing were initially thought to support a “task-positive” model, whereas recent RS-fMRI studies have begun to explore the roles of “task-negative” regions and networks in more general cognitive functioning (Whitfield-Gabrieli & Ford, 2012). As subsequently discussed, our results indicate that different measures of LFFs provide novel insights into how “task-positive” and “task-negative” regions and networks contribute to spoken language learning.

4.1. Regional spontaneous activity and spoken language learning ability

Using an ALFF analysis that was sensitive to regional variations in spontaneous activity, we observed that regional spontaneous brain activities correlated with learning throughout various brain regions of the frontal, temporal, and parietal areas. Our two key findings are detailed as follows.

First, ALFF values in the LSTG were positively correlated with Generalization scores. This region has been proposed to be involved in acoustic-phonetic mapping in recent dual stream models of speech processing (Hickok & Poeppel, 2007; Rauschecker & Scott, 2009). Furthermore, the LSTG appears to be a computational hub within the language network wherein phonological and semantic information interface. In our previous task-based fMRI

study, participants discriminated pitch patterns of words before and after they were trained to learn the words. Increased BOLD activation was observed in the LSTG following training in the successful learners more so than in the less successful learners (Wong et al., 2007); these findings are indicative of the important role of this region in the integration of phonetic features (e.g., pitch patterns) into words. Using the same training procedure employed in the present study, our previous diffusion MRI study highlighted the potential structural significance of the LSTG in sound-to-word learning by revealing an extreme capsule ventral pathway composed of an inferior longitudinal fasciculus branch that runs along the LSTG. Within this pathway, the white matter fractional anisotropy was correlated with sound-to-word learning success (Wong et al., 2011). Furthermore, the role of the LSTG in novel-sound learning might depend on lexical context. For example, several cross-linguistic studies have identified the left IFG as a crucial region for the processing of pitch in a non-lexical context (Wong, Parsons, Martinez, & Diehl, 2004). However, ALFF values of the left IFG were not correlated with learning performance, which further emphasizes the specific contribution of the LSTG to learning in a true lexical context (e.g., a word context, Wong et al., 2007). Future studies should investigate the functional dissociation between the left IFG and the LSTG in learning novel sounds in different contexts.

Second, negative correlations between ALFF values and Generalization scores were observed in several clusters, including PCUN/PCG, RITG, ORBmid, RSFGdor, RACG/LSFGmed, RANG/RMTG, RIPL/LANG and RSFGmed. The DMN is composed of a group of large but widely separated clusters (e.g., PCUN/PCG, RITG, ORBmid, RANG/RMTG, RIPL/LANG) located in the core DMN regions (Buckner, Andrews-Hanna, & Schacter, 2008; Whitfield-Gabrieli & Ford, 2012). Although the ACG and SFG do not belong to the core DMN, they were identified as extended DMN regions in an affective reappraisal task (Sheline et al., 2009). Thus, all these clusters with negative correlations were considered DMN regions. The brain activities in these regions are greater during rest than during engagement in goal-oriented tasks, which indicates that DMN deactivation is required for the performance of tasks (Buckner et al., 2008). Consistent with this view, a recent task-based fMRI study demonstrated that slower target response times were preceded by greater DMN activation during a classic vigilance task (Hinds et al., 2013). Although DMN activation was observed in the pre-stimulus period rather than in the resting-state, the findings of Hinds et al. (2013) indicate that DMN activity reflects the ability to process task-related stimuli to enable optimal performance. Our results demonstrate that successful learning benefits from low levels of spontaneous activity in DMN regions during a task-free period without task engagement. Our results also suggest that for the acquisition of novel, complex sounds, successful learning requires the learner to *deactivate* the DMN.

Our finding that regional spontaneous activity measure can be used to predict language learning capacities is of particular importance in the context of the investigation of neural predictors of spoken language learning. First, various methods for defining ROIs have been widely used in previous resting-state studies (Baldassarre et al., 2012; Supekar et al., 2013; Ventura-Campos et al., 2013). Through the application of regional measures without prior ROIs, inconsistencies produced by the different methods can be ruled out. Second, although rsFC is widely used (Baldassarre et al., 2012; Lewis, Baldassarre, Committeri, Romani, &

Corbetta, 2009; Supekar et al., 2013; Vahdat, Darainy, Milner, & Ostry, 2011; Ventura-Campos et al., 2013), it remains difficult to draw conclusions from the specific regions that contribute to learning because rsFC reflects synchronization between two regions rather than the regional activity within a specific region. Through the examination of ALFFs, regional measures can be used as the first step for investigations of the neural predictors of spoken language learning at the regional level.

4.2. Graph theory-based measures and spoken language learning ability

Several RS-fMRI studies have demonstrated learning-related changes in functional connectivity, and the authors have discussed the relationships of these changes with learning capacity. However, a direct link between intrinsic and whole-brain functional connectivity and individual differences in learning capacity has not been observed. In the present study, graph theory-based approaches were implemented to examine the extent to which the topological properties of specific regions and the global network could be used to infer spoken language learning. Although we did not observe significant correlations between global network measures and Generalization scores, our exploratory analysis revealed that nodal efficiency, nodal degree and nodal betweenness for some significant ALFF-analysis regions (e.g., LSTG, LANG, LPCG and PCUN) correlated with Generalization scores. These effects are generally consistent with the findings of RS-fMRI studies, which indicate that nodal measures are associated with individual differences in variables such as aging, pathological disease and cognitive processes (Wang et al., 2010). Both nodal degree and nodal efficiency reflect the importance of individual regions in the whole network, and the greater nodal efficiency of this region implies more rapid transmission of information between that region and the global network. The observation that increased nodal degree and nodal efficiency in the LSTG were associated with improved learning capacity indicates that individuals with more information integration in the LSTG would show greater potential for sound-to-word learning. We also observed nodal measures in some DMN regions (e.g., LANG, LPCG and PCUN) were negatively correlated with Generalization scores. The correlations pattern converged with our ALFF results in that the ALFF of LSTG was found to be positively correlated with learning, whereas the ALFFs of those DMN regions were negatively correlated with learning. Thus, these findings further support the idea that learning might benefit from emphasizing task-related regions and de-emphasizing DMN regions. Taken together, these results suggest that the intrinsic cortical network is organized in a specific manner; high local efficiency and strengthened connections in task-related regions and weakened connections DMN regions may improve the acquisition of a foreign language.

Given that global measures, such as global and local efficiencies, have been associated with task performance (Sheppard et al., 2011; L. Wang, Li, Metzak, He, & Woodward, 2010) in task-fMRI data and pathological disease in RS-fMRI data (Bassett & Bullmore, 2009), it was surprising that global measures, such as E_{global}, E_{local}, did not correlate with learning capacity in our data. One potential explanation for the absence of these correlations is that the participants in our study were healthy adults, and the global brain network at rest is topologically stable and similar across the participants. Thus, the global measures might not have been sufficiently sensitive to detect the variations in learning capacity.

4.3. Network interactions and spoken language learning ability

RS-fMRI studies have consistently demonstrated that the human brain is organized into several large-scale distributed networks. Using ICA, in the present study, several RSNs were identified in a data-driven manner. Anticorrelated interactions between the DMN and other RSNs are commonly interpreted as "competition" (Fox et al., 2005). The DMN exhibited anticorrelation with the other RSNs, with the exception of the visual network (e.g., VN); these findings are consistent with the concept that competition between two large systems, e.g., the DMN and the task-positive system, is reflected in spontaneous or intrinsic brain dynamics.

The concept of "competition" has been shown to support normal cognitive functioning (Castellanos et al., 2008; Whitfield-Gabrieli et al., 2009) and to reflect individual variations in task performance (Fornito et al., 2012; Kelly et al., 2008). Specifically, one of the attention networks (e.g., DAN) is hypothesized to modulate externally directed attention via top-down orienting (Corbetta & Shulman, 2002; Ptak & Schnider, 2010), whereas the DMN is associated with internal cognitive processes and deactivates during orienting driven by the external environment (Greicius, Krasnow, Reiss, & Menon, 2003). This opposing pattern might represent a hallmark of normal brain functioning (Whitfield-Gabrieli & Ford, 2012). In our data, the association between better learning performance and a weaker anticorrelation between the DMN and DAN speaks against the hypothesis that a greater separation (i.e., stronger anticorrelation) of the DMN and task-positive networks, such as DAN, should enhance task performance. This hypothesis has been supported by evidence that stronger anticorrelations (*r* values that approach −1) between the DMN and the task-positive attention network are associated with less variable task performance (Kelly et al., 2008). However, the functional significance of the co-activation or "cooperation" (*r* values approach 1) between these networks has been demonstrated in recent works (Christoff, Gordon, Smallwood, Smith, & Schooler, 2009; Fornito et al., 2012; Prado & Weissman, 2011). Prado and Weissman (2011) noted that less variable performances might indicate less improvement or less deterioration of behavior; the authors indicated that an increased "cooperation" (*r* values approach 1) between DMN region and task-positive attention network regions is associated with increased response times (RTs) in the current trial (i.e., poor performance) and deceased RTs in the next trial (i.e., enhanced performance) in a selective attention task. These authors hypothesized that the degree of anticorrelation between the DMN and the task-positive networks supports current task performance, whereas the degree of co-activation between these networks reflects performance improvement. In the context of learning a new skill, compared with less successful learners, successful learners typically achieve greater progress after they receive the same period of training. This difference might explain why we observed that weaker, not stronger anticorrelations between the DMN and the DAN, were associated with higher Generalization scores in our data. Our findings suggest that this weaker anticorrelation might reflect the cognitive system's ability to make adaptive changes (Prado & Weissman, 2011) that are essential for learning.

Notably, our findings were based on RS-fMRI data, and network interactions might exhibit covariations in different contexts (Fornito et al., 2012). It is unclear whether the relationship

between the DMN-DAN interaction and learning capacity is consistent across resting and task conditions. Future studies that combine resting-state and task-based fMRI may further elucidate the nature of this relationship by examining whether it is altered in different resting-states (e.g., eyes-closed and open) and task-states (e.g., learning-related and learning-unrelated tasks).

4.4. Limitations

In searching for converging evidence through multiple analytical methods, several decisions regarding the analyses may have influenced our results. First, for the graph theory-based analyses, we chose not to regress out the global mean signal to avoid negative FCs and anticorrelations between regions (Rubinov & Sporns, 2010). For the network interaction analyses, we chose to regress out the global mean signal to investigate the anticorrelations between RSNs (Fox et al., 2005). The inconsistency in the handling of the global mean signal might lead to controversies regarding the explanation of the anticorrelation results (Fox, Zhang, Snyder, & Raichle, 2009; Murphy, Birn, Handwerker, Jones, & Bandettini, 2009). We note that our graph theory-based analysis was independent of our network interaction analyses, and these analyses focused on different aspects of the brain networks. To avoid negative correlations produced by global mean signal removal (Murphy et al., 2009), we did not regress out the global mean signal in our graph theory-based anlaysis (Rubinov & Sporns, 2010). However, global mean signal removal has been shown to be effective in removing physiological noise and improving FC specificity when anticorrelated RSNs (Fornito et al., 2012; Fox et al., 2005; Weissenbacher et al., 2009), such as the DMN and DAN, are considered. Consequently, in our opinion, it is reasonable that global mean signal removal was applied selectively in the network interaction analyses but not in our graph theory-based analyses. Additional work that applies approaches that remove physiological noise without global mean signal removal is needed to determine the robustness of the anticorrelated RSNs that were identified in the current work.

Although ALFF has been widely applied in RS-fMRI studies, the nature of ALFF in cognitive performance remains unclear. By definition, ALFF measures the brain signal variability (variance) in the frequency domain. However, traditional analysis method of task-fMRI is based on the mean signal in the time domain. It is possible that ALFF captures different aspects of brain signals that task-fMRI studies are not able to uncover. Future studies will need to combine task-based fMRI and RS-fMRI to reveal different aspects of brain signaling in cognitive performance.

Third, the graph theory-based analysis and the internetwork connectivity analysis results did not pass the corrected threshold. Thus, those results should be treated as exploratory. However, we found that different RS-fMRI parameters (e.g., ALFF and nodal measures) in the LSTG correlated with learning success. Future studies will need to apply voxel-wise graph theory-based analysis and examine whether ALFF analysis results and graph theory-based analysis results would converge.

Fourth, our relatively small sample size may undermine the reliability and robustness of our results. Future studies will need to apply a larger sample size to further assess the stability of

the relationship between learning performance and the RS-fMRI measures we used in the current study.

5. Conclusions

By using RS-fMRI to investigate the neural predictors of individual differences in spoken language learning, we demonstrated that sound-to-word learning success is predicted by the regional spontaneous activities of "task-positive" regions, such as LSTG, and "task-negative" network regions. Furthermore, we demonstrated that the topological properties of the LSTG are associated with learning. Finally, we obtained evidence that inter-network interactions predict learning. Taken together, the results of the present study support the claim of the STR hypothesis that distinct LFF patterns reflect individual differences in behavior by showing different RS-fMRI measures that predict learning success. The results also indicate that different measures of spontaneous brain activity provide complementary information, and extend our understanding of the nature of spontaneous brain activity and individual variations in learning and adaptive behavior. More importantly, the results provide evidence that individual differences in spoken learning success can be predicted objectively and without guidance of task-related fMRI and prior hypotheses. Because the RS-fMRI does not require a task, it can be ideal for studies on clinical population who are unable to perform complex tasks. RS-fMRI might also represent a useful screening method for evaluating disease-related pathology because it can be conducted over a short period without a fMRI localizer task.

Supplementary Material

Refer to Web version on PubMed Central for supplementary material.

Acknowledgments

We would like to thank Oliver Bones and John Patrick Sheppard for comments on drafts of this manuscript. We would also like to thank two anonymous reviewers for their helpful comments and constructive critique.

Funding

This work was supported by the U.S. National Institutes of Health grants (R01DC008333 and R01DC013315), the Research Grants Council of Hong Kong grants (477513 and 14117514), the Health and Medical Research Fund of Hong Kong grant (01120616), and the Dr. Stanley Ho Medical Development Foundation to P.C.M.W., by the Key Project of National Social Science Foundation of China (15AZD048) and the Key Project of National Natural Science Foundation of Guangdong Province (2014A030311016) to S.W., by the U.S. National Institutes of Health grant (R01DC013315) to B.C. and by the Guangzhou Elites Project of Guangzhou Municipal Government (JY201245) to Z.D.

REFERENCES

Achard S, Bullmore E. Efficiency and cost of economical brain functional networks. PLoS Computational Biology. 2007; 3(2):e17. http://dx.doi.org/10.1371/journal.pcbi.0030017. [PubMed: 17274684]

Baldassarre A, Lewis CM, Committeri G, Snyder AZ, Romani GL, Corbetta M. Individual variability in functional connectivity predicts performance of a perceptual task. Proceedings of the National Academy of Sciences of the United States of America. 2012; 109(9):3516–3521. http://dx.doi.org/10.1073/pnas.1113148109. [PubMed: 22315406]

Bassett DS, Bullmore ET. Human brain networks in health and disease. Current Opinion in Neurology. 2009; 22(4):340–347. http://dx.doi.org/10.1097/WCO.0b013-32832d93dd. [PubMed: 19494774]

Biswal B, Yetkin FZ, Haughton VM, Hyde JS. Functional connectivity in the motor cortex of resting human brain using echo-planar MRI. Magnetic Resonance in Medicine. 1995; 34(4):537–541. [PubMed: 8524021]

Brown, L.; Sherbenou, RJ.; Johnsen, SK. TONI-3: Test of nonverbal intelligence. 3rd ed.. Pro-Ed; Austin, TX: 1997.

Buckner RL, Andrews-Hanna JR, Schacter DL. The brain's default network – anatomy, function, and relevance to disease. Year in Cognitive Neuroscience. 2008; 1124:1–38. http://dx.doi.org/10.1196/annals.1440.011.

Bullmore E, Sporns O. Complex brain networks: graph theoretical analysis of structural and functional systems. Nature Reviews Neuroscience. 2009; 10(3):186–198. http://dx.doi.org/10.1038/nrn2575. [PubMed: 19190637]

Castellanos FX, Margulies DS, Kelly C, Uddin LQ, Ghaffari M, Kirsch A, et al. Cingulate-precuneus interactions: a new locus of dysfunction in adult attention-deficit/hyperactivity disorder. Biological Psychiatry. 2008; 63(3):332–337. http://dx.doi.org/10.1016/j.biopsych.2007.06.025. [PubMed: 17888409]

Chandrasekaran B, Kraus N, Wong PC. Human inferior colliculus activity relates to individual differences in spoken language learning. Journal of Neurophysiology. 2012; 107(5):1325–1336. http://dx.doi.org/10.1152/jn.00923.2011. [PubMed: 22131377]

Chandrasekaran B, Sampath PD, Wong PCM. Individual variability in cue-weighting and lexical tone learning. Journal of the Acoustical Society of America. 2010; 128(1):456–465. http://dx.doi.org/10.1121/1.3445785. [PubMed: 20649239]

Chandrasekaran B, Yi HG, Blanco NJ, McGeary JE, Maddox WT. Enhanced procedural learning of speech sound categories in a genetic variant of FOXP2. Journal of Neuroscience. 2015; 35(20):7808–7812. http://dx.doi.org/10.1523/JNEUROSCI.4706-14.2015. [PubMed: 25995468]

Chao-Gan Y, Yu-Feng Z. DPARSF: a MATLAB toolbox for “Pipeline” data analysis of resting-state fMRI. Frontiers in Systems Neuroscience. 2010; 4:13. http://dx.doi.org/10.3389/fnsys.2010.00013. [PubMed: 20577591]

Christoff K, Gordon AM, Smallwood J, Smith R, Schooler JW. Experience sampling during fMRI reveals default network and executive system contributions to mind wandering. Proceedings of the National Academy of Sciences of the United States of America. 2009; 106(21):8719–8724. http://dx.doi.org/10.1073/pnas.0900234106. [PubMed: 19433790]

Corbetta M, Shulman GL. Control of goal-directed and stimulus-driven attention in the brain. Nature Reviews Neuroscience. 2002; 3(3):201–215. http://dx.doi.org/10.1038/Nrn755. [PubMed: 11994752]

Fornito A, Harrison BJ, Zalesky A, Simons JS. Competitive and cooperative dynamics of large-scale brain functional networks supporting recollection. Proceedings of the National Academy of Sciences of the United States of America. 2012; 109(31):12788–12793. http://dx.doi.org/10.1073/pnas.1204185109. [PubMed: 22807481]

Fornito A, Zalesky A, Bullmore ET. Network scaling effects in graph analytic studies of human resting-state FMRI data. Frontiers in Systems Neuroscience. 2010; 4:22. [PubMed: 20592949]

Fox MD, Raichle ME. Spontaneous fluctuations in brain activity observed with functional magnetic resonance imaging. Nature Reviews Neuroscience. 2007; 8(9):700–711. http://dx.doi.org/10.1038/Nrn2201. [PubMed: 17704812]

Fox MD, Snyder AZ, Vincent JL, Corbetta M, Van Essen DC, Raichle ME. The human brain is intrinsically organized into dynamic, anticorrelated functional networks. Proceedings of the National Academy of Sciences of the United States of America. 2005; 102(27):9673–9678. http://dx.doi.org/10.1073/pnas.0504136102. [PubMed: 15976020]

Fox MD, Zhang DY, Snyder AZ, Raichle ME. The global signal and observed anticorrelated resting state brain networks. Journal of Neurophysiology. 2009; 101(6):3270–3283. http://dx.doi.org/10.1152/jn.90777.2008. [PubMed: 19339462]

Freeman LC. A set of measures of centrality based on betweenness. Sociometry. 1997; 40:35–41.

Friston KJ. Functional and effective connectivity: a review. Brain Connectivity. 2011; 1(1):13–36. http://dx.doi.org/10.1089/brain.2011.0008. [PubMed: 22432952]

Geranmayeh F, Wise RJ, Mehta A, Leech R. Overlapping networks engaged during spoken language production and its cognitive control. The Journal of Neuroscience: the Official Journal of the Society for Neuroscience. 2014; 34:8728–8740. [PubMed: 24966373]

Golestani N, Zatorre RJ. Individual differences in the acquisition of second language phonology. Brain and Language. 2009; 109(2–3):55–67. http://dx.doi.org/10.1016/j.bandl.2008.01.005. [PubMed: 18295875]

Greicius MD, Krasnow B, Reiss AL, Menon V. Functional connectivity in the resting brain: a network analysis of the default mode hypothesis. Proceedings of the National Academy of Sciences of the United States of America. 2003; 100(1):253–258. http://dx.doi.org/10.1073/pnas.0135058100. [PubMed: 12506194]

Harmelech T, Malach R. Neurocognitive biases and the patterns of spontaneous correlations in the human cortex. Trends in Cognitive Sciences. 2013; 17:606–615. [PubMed: 24182697]

Hickok G, Poeppel D. Opinion e the cortical organization of speech processing. Nature Reviews Neuroscience. 2007; 8(5):393–402. http://dx.doi.org/10.1038/Nrn2113. [PubMed: 17431404]

Hinds O, Thompson TW, Ghosh S, Yoo JJ, Whitfield-Gabrieli S, Triantafyllou C, et al. Roles of default-mode network and supplementary motor area in human vigilance performance: evidence from real-time fMRI. Journal of Neurophysiology. 2013; 109(5):1250–1258. http://dx.doi.org/10.1152/jn.00533.2011. [PubMed: 23236006]

Kelly AMC, Uddin LQ, Biswal BB, Castellanos FX, Milham MP. Competition between functional brain networks mediates behavioral variability. NeuroImage. 2008; 39(1):527–537. http://dx.doi.org/10.1016/j.neuroimage.2007.08.008. [PubMed: 17919929]

Latora V, Marchiori M. Efficient behavior of small-world networks. Physical Review Letters. 2001; 87(19):198701. [PubMed: 11690461]

Lewis CM, Baldassarre A, Committeri G, Romani GL, Corbetta M. Learning sculpts the spontaneous activity of the resting human brain. Proceedings of the National Academy of Sciences of the United States of America. 2009; 106(41):17558–17563. http://dx.doi.org/10.1073/pnas.0902455106. [PubMed: 19805061]

Lively SE, Logan JS, Pisoni DB. Training Japanese listeners to identify English /r/and /l/. II: The role of phonetic environment and talker variability in learning new perceptual categories. The Journal of the Acoustical Society of America. 1993; 94:1242–1255. [PubMed: 8408964]

Malaia E, Talavage TM, Wilbur RB. Functional connectivity in task-negative network of the deaf: effects of sign language experience. PeerJ. 2014; 2:e446. http://dx.doi.org/10.7717/peerj.446. [PubMed: 25024915]

Marcotte K, Perlbarg V, Marrelec G, Benali H, Ansaldo AI. Default-mode network functional connectivity in aphasia: therapy-induced neuroplasticity. Brain and Language. 2013; 124:45–55. [PubMed: 23274798]

Marian V, Blumenfeld HK, Kaushanskaya M. The Language Experience and Proficiency Questionnaire (LEAP-Q): assessing language profiles in bilinguals and multilinguals. Journal of Speech Language and Hearing Research. 2007; 50(4):940–967. http://dx.doi.org/10.1044/1092-4388(2007/067).

Mennes M, Zuo XN, Kelly C, Di Martino A, Zang YF, Biswal B, et al. Linking inter-individual differences in neural activation and behavior to intrinsic brain dynamics. NeuroImage. 2011; 54(4):2950–2959. http://dx.doi.org/10.1016/j.neuroimage.2010.10.046. [PubMed: 20974260]

Mueller S, Wang D, Fox MD, Yeo BT, Sepulcre J, Sabuncu MR, et al. Individual variability in functional connectivity architecture of the human brain. Neuron. 2013; 77(3):586–595. http://dx.doi.org/10.1016/j.neuron.2012.12.028. [PubMed: 23395382]

Murphy K, Birn RM, Handwerker DA, Jones TB, Bandettini PA. The impact of global signal regression on resting state correlations: are anti-correlated networks introduced? NeuroImage. 2009; 44(3):893–905. http://dx.doi.org/10.1016/j.neuroimage.2008.09.036. [PubMed: 18976716]

Prado J, Weissman DH. Heightened interactions between a key default-mode region and a key task-positive region are linked to suboptimal current performance but to enhanced future performance.

NeuroImage. 2011; 56(4):2276–2282. http://dx.doi.org/10.1016/j.neuroimage.2011.03.048. [PubMed: 21440073]

Ptak R, Schnider A. The dorsal attention network mediates orienting toward behaviorally relevant stimuli in spatial neglect. Journal of Neuroscience. 2010; 30(38):12557–12565. http://dx.doi.org/10.1523/Jneurosci.2722-10.2010. [PubMed: 20861361]

Rauschecker JP, Scott SK. Maps and streams in the auditory cortex: nonhuman primates illuminate human speech processing. Nature Neuroscience. 2009; 12(6):718–724. http://dx.doi.org/10.1038/nn.2331. [PubMed: 19471271]

Rissanen J. Modeling by shortest data description. Automatica. 1978; 14(5):465–471. http://dx.doi.org/10.1016/0005-1098(78)90005-5.

Rubinov M, Sporns O. Complex network measures of brain connectivity: uses and interpretations. NeuroImage. 2010; 52(3):1059–1069. http://dx.doi.org/10.1016/j.neuroimage.2009.10.003. [PubMed: 19819337]

Sanz-Arigita EJ, Schoonheim MM, Damoiseaux JS, Rombouts SA, Maris E, Barkhof F, et al. Loss of 'small-world' networks in Alzheimer's disease: graph analysis of FMRI resting-state functional connectivity. PLoS One. 2010; 5(11):e13788. http://dx.doi.org/10.1371/journal.pone.0013788. [PubMed: 21072180]

Sheline YI, Barch DM, Price JL, Rundle MM, Vaishnavi SN, Snyder AZ, et al. The default mode network and self-referential processes in depression. Proceedings of the National Academy of Sciences of the United States of America. 2009; 106:1942–1947. [PubMed: 19171889]

Sheppard JP, Wang JP, Wong PC. Large-scale cortical functional organization and speech perception across the lifespan. PLoS One. 2011; 6(1):e16510. http://dx.doi.org/10.1371/journal.pone.0016510. [PubMed: 21304991]

Sheppard JP, Wang JP, Wong PCM. Large-scale cortical network properties predict future sound-to-word learning success. Journal of Cognitive Neuroscience. 2012; 24(5):1087–1103. [PubMed: 22360625]

Smith SM, Fox PT, Miller KL, Glahn DC, Fox PM, Mackay CE, et al. Correspondence of the brain's functional architecture during activation and rest. Proceedings of the National Academy of Sciences of the United States of America. 2009; 106(31):13040–13045. http://dx.doi.org/10.1073/pnas.0905267106. [PubMed: 19620724]

Song XW, Dong ZY, Long XY, Li SF, Zuo XN, Zhu CZ, et al. REST: a toolkit for resting-state functional magnetic resonance imaging data processing. PLos One. 2011; 6(9) http://dx.doi.org/10.1371/journal.pone.0025031.

Supekar K, Swigart AG, Tenison C, Jolles DD, Rosenberg-Lee M, Fuchs L, et al. Neural predictors of individual differences in response to math tutoring in primary-grade school children. Proceedings of the National Academy of Sciences of the United States of America. 2013; 110(20):8230–8235. http://dx.doi.org/10.1073/pnas.1222154110. [PubMed: 23630286]

Tzourio-Mazoyer N, Landeau B, Papathanassiou D, Crivello F, Etard O, Delcroix N, et al. Automated anatomical labeling of activations in SPM using a macroscopic anatomical parcellation of the MNI MRI single-subject brain. NeuroImage. 2002; 15(1):273–289. http://dx.doi.org/10.1006/nimg.2001.0978. [PubMed: 11771995]

Vahdat S, Darainy M, Milner TE, Ostry DJ. Functionally specific changes in resting-state sensorimotor networks after motor learning. Journal of Neuroscience. 2011; 31(47):16907–16915. http://dx.doi.org/10.1523/JNEUROSCI.2737-11.2011. [PubMed: 22114261]

Ventura-Campos N, Sanjuan A, Gonzalez J, Palomar-Garcia MA, Rodriguez-Pujadas A, Sebastian-Galles N, et al. Spontaneous brain activity predicts learning ability of foreign sounds. Journal of Neuroscience. 2013; 33(22):9295–9305. http://dx.doi.org/10.1523/JNEUROSCI.4655-12.2013. [PubMed: 23719798]

Wang X, Han Z, He Y, Caramazza A, Song L, Bi Y. Where color rests: spontaneous brain activity of bilateral fusiform and lingual regions predicts object color knowledge performance. NeuroImage. 2013; 76:252–263. http://dx.doi.org/10.1016/j.neuroimage.2013.03.010. [PubMed: 23518009]

Wang L, Li YF, Metzak P, He Y, Woodward TS. Age-related changes in topological patterns of large-scale brain functional networks during memory encoding and recognition. NeuroImage. 2010; 50(3):862–872. http://dx.doi.org/10.1016/j.neuroimage.2010.01.044. [PubMed: 20093190]

Wang Y, Spence MM, Jongman A, Sereno JA. Training American listeners to perceive Mandarin tones. Journal of the Acoustical Society of America. 1999; 106(6):3649–3658. [PubMed: 10615703]

Wang J, Zuo X, He Y. Graph-based network analysis of resting-state functional MRI. Frontiers in Systems Neuroscience. 2010; 4:16. http://dx.doi.org/10.3389/fnsys.2010.00016. [PubMed: 20589099]

Wei T, Liang X, He Y, Zang Y, Han Z, Caramazza A, et al. Predicting conceptual processing capacity from spontaneous neuronal activity of the left middle temporal gyrus. Journal of Neuroscience. 2012; 32(2):481–489. http://dx.doi.org/10.1523/JNEUROSCI.1953-11.2012. [PubMed: 22238084]

Weissenbacher A, Kasess C, Gerstl F, Lanzenberger R, Moser E, Windischberger C. Correlations and anticorrelations in resting-state functional connectivity MRI: a quantitative comparison of preprocessing strategies. NeuroImage. 2009; 47(4):1408–1416. http://dx.doi.org/10.1016/j.neuroimage.2009.05.005. [PubMed: 19442749]

Whitfield-Gabrieli S, Ford JM. Default mode network activity and connectivity in Psychopathology. Annual Review of Clinical Psychology. 2012; 8(8):49–+. http://dx.doi.org/10.1146/annurevclinpsy-032511-143049.

Whitfield-Gabrieli S, Thermenos HW, Milanovic S, Tsuang MT, Faraone SV, McCarley RW, et al. Hyperactivity and hyperconnectivity of the default network in schizophrenia and in first-degree relatives of persons with schizophrenia. Proceedings of the National Academy of Sciences of the United States of America. 2009; 106(4):1279–1284. http://dx.doi.org/10.1073/pnas.0809141106. [PubMed: 19164577]

Wong FCK, Chandrasekaran B, Garibaldi K, Wong PCM. White matter anisotropy in the ventral language pathway predicts sound-to-word learning Success. Journal of Neuroscience. 2011; 31(24):8780–8785. http://dx.doi.org/10.1523/Jneurosci.0999-11.2011. [PubMed: 21677162]

Wong PCM, Chandrasekaran B, Zheng J. The derived allele of ASPM is associated with lexical tone perception. PLoS One. 2012; 7(4):e34243. http://dx.doi.org/10.1371/journal.pone.0034243. [PubMed: 22529908]

Wong PCM, Parsons LM, Martinez M, Diehl RL. The role of the insular cortex in pitch pattern perception: the effect of linguistic contexts. Journal of Neuroscience. 2004; 24(41):9153–9160. http://dx.doi.org/10.1523/JNEUROSCI.2225-04.2004. [PubMed: 15483134]

Wong PCM, Perrachione TK. Learning pitch patterns in lexical identification by native English-speaking adults. Applied Psycholinguistics. 2007; 28(4):565–585. http://dx.doi.org/10.1017/S0142716407070312.

Wong PCM, Perrachione TK, Parrish TB. Neural characteristics of successful and less successful speech and word learning in adults. Human Brain Mapping. 2007; 28(10):995–1006. http://dx.doi.org/10.1002/hbm.20330. [PubMed: 17133399]

Woodcock, RW.; McGrew, KS.; Mather, N. Woodcock-Johnson III tests of cognitive abilities. Riverside Publishing; Itasca, IL: 2001.

Xia M, Wang J, He Y. BrainNet Viewer: a network visualization tool for human brain connectomics. PloS one. 2013; 8:e68910. [PubMed: 23861951]

Yi, HG.; Maddox, WT.; Mumford, JA.; Chandrasekaran, B. The role of corticostriatal systems in speech category learning.. Cerebral Cortex. 2014. http://dx.doi.org/10.1093/cercor/bhu236

Zalesky A, Fornito A, Harding IH, Cocchi L, Yucel M, Pantelis C, et al. Whole-brain anatomical networks: does the choice of nodes matter? NeuroImage. 2010; 50:970–983. [PubMed: 20035887]

Zang YF, He Y, Zhu CZ, Cao QJ, Sui MQ, Liang M, et al. Altered baseline brain activity in children with ADHD revealed by resting-state functional MRI. Brain & Development. 2007; 29(2):83–91. http://dx.doi.org/10.1016/j.braindev.2006.07.002. [PubMed: 16919409]

Zatorre RJ. Predispositions and plasticity in music and speech learning: neural correlates and implications. Science. 2013; 342(6158):585–589. http://dx.doi.org/10.1126/science.1238414. [PubMed: 24179219]

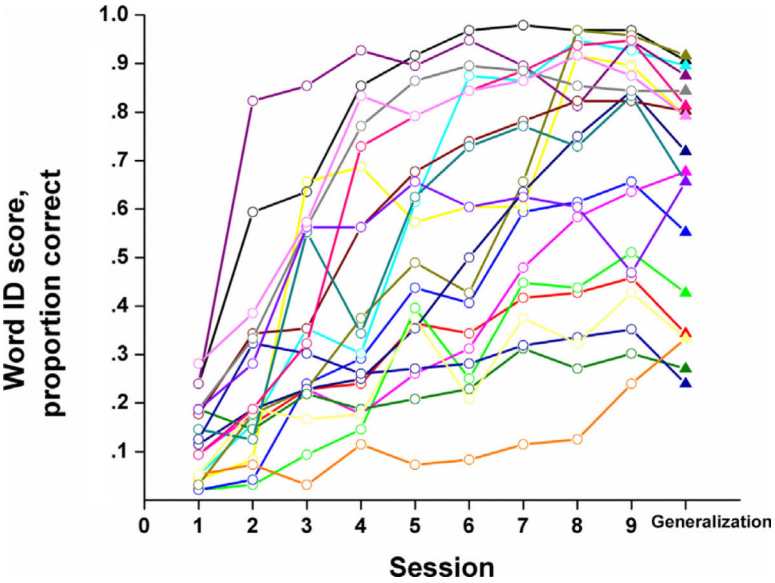

Fig. 1.
The language learning curves over the nine-day training-session.

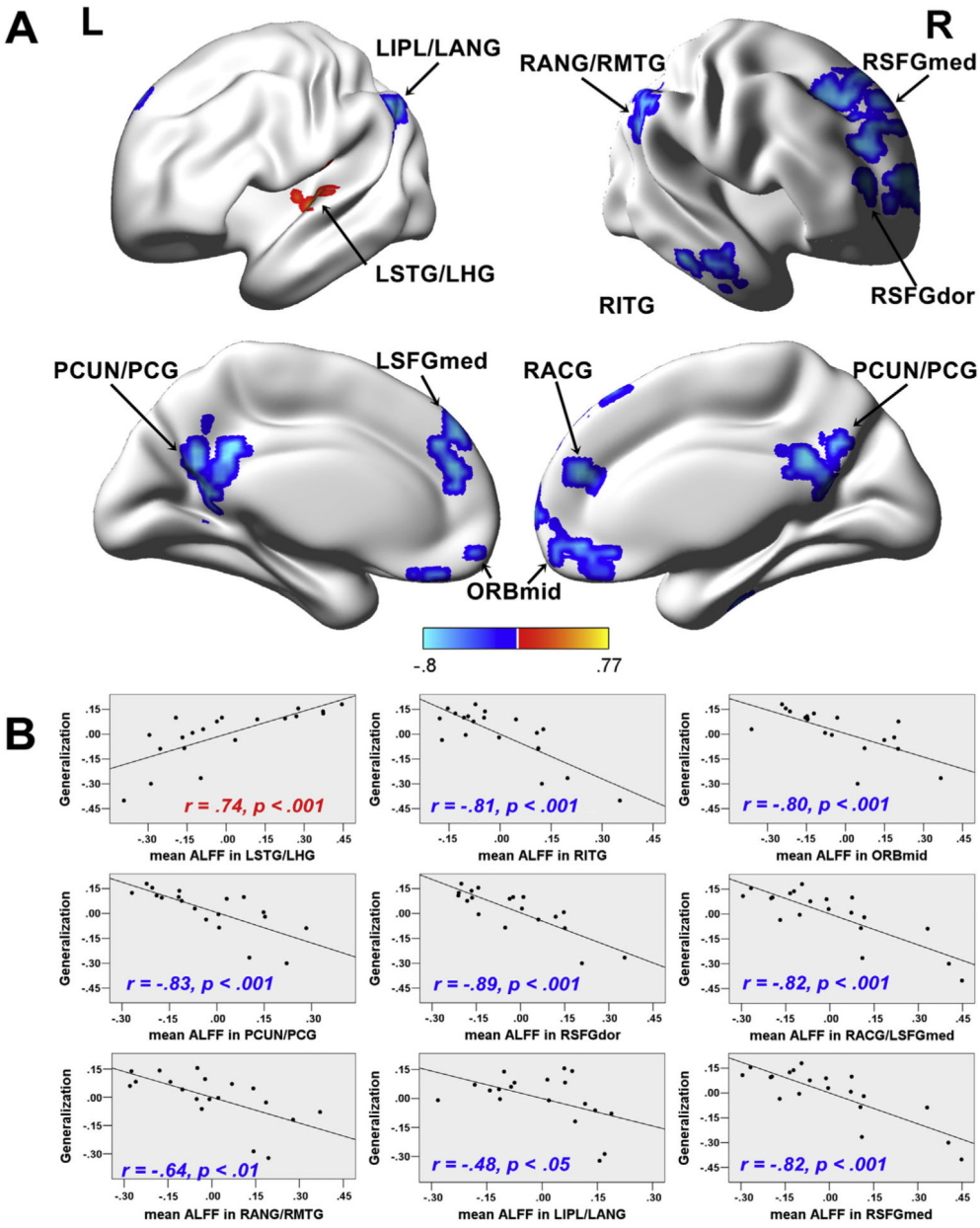

Fig. 2.

ALFF-behavior correlation analyses. A) Statistical maps of partial correlations between ALFF values and Generalization scores after controlling for the effects of Tone ID and IQ ($p < .05$, corrected by AlphaSim with cluster size > 54 voxels). The ALFF values were mapped on the cortical surface by using BrainNet Viewer (Xia, Wang, & He, 2013). The correlation r value is presented by the color bar at the bottom. L: left; R: right. B) Scatter plots showing partial correlations between the mean ALFF within each region plotted in A and Generalization scores after controlling for the effects of Tone ID and IQ. For the RANG/MTG and the LIPL/LANG clusters, one extreme data point was removed. Before data point removal, the correlation value was −.78 and −.68 for the RANG/MTG and the LIP/LANG, respectively.

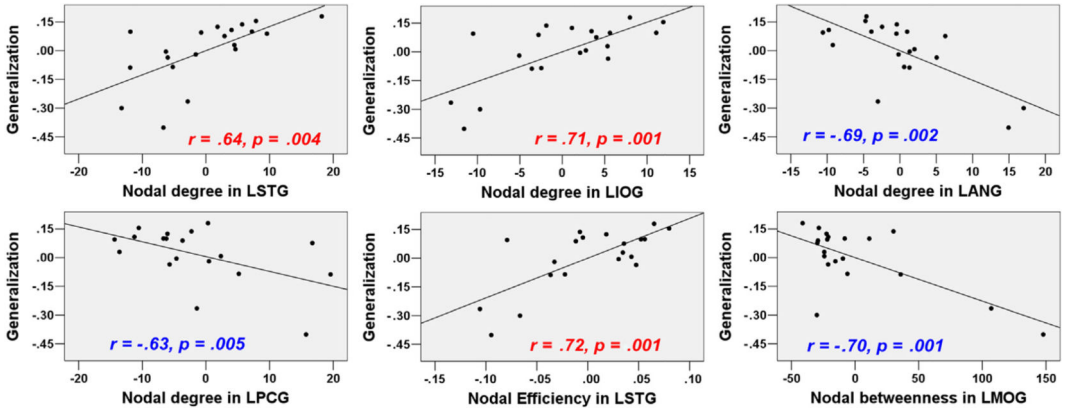

Fig. 3.

Correlations between nodal network measures (AAL-90) and Generalization scores after controlling for the effects of Tone ID and IQ (data without global signal regression; uncorrected $p < .005$).

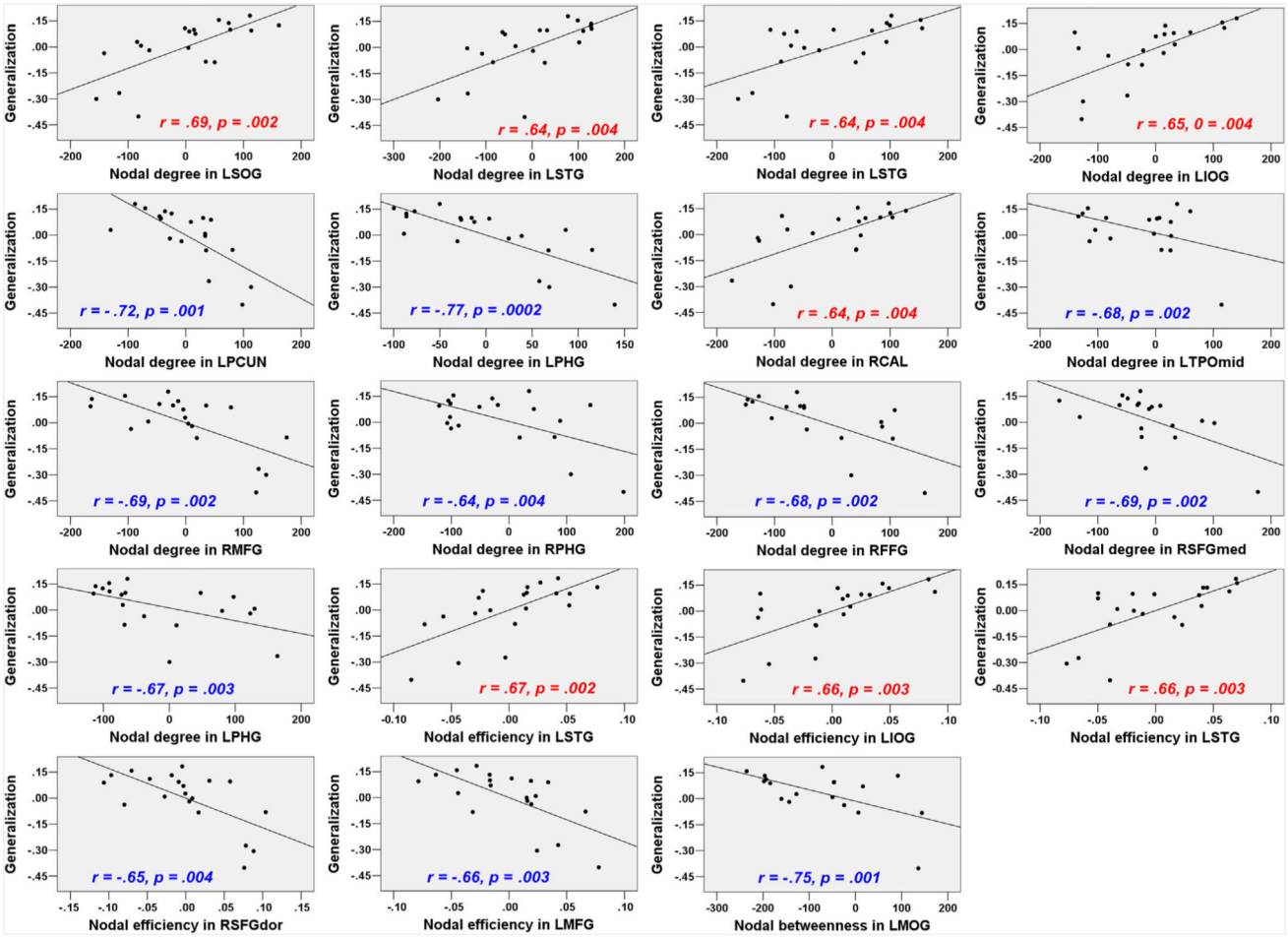

Fig. 4.

Correlations between nodal network measures (AAL-1024) and Generalization scores after controlling for the effects of Tone ID and IQ (data without global signal regression; uncorrected $p < .005$).

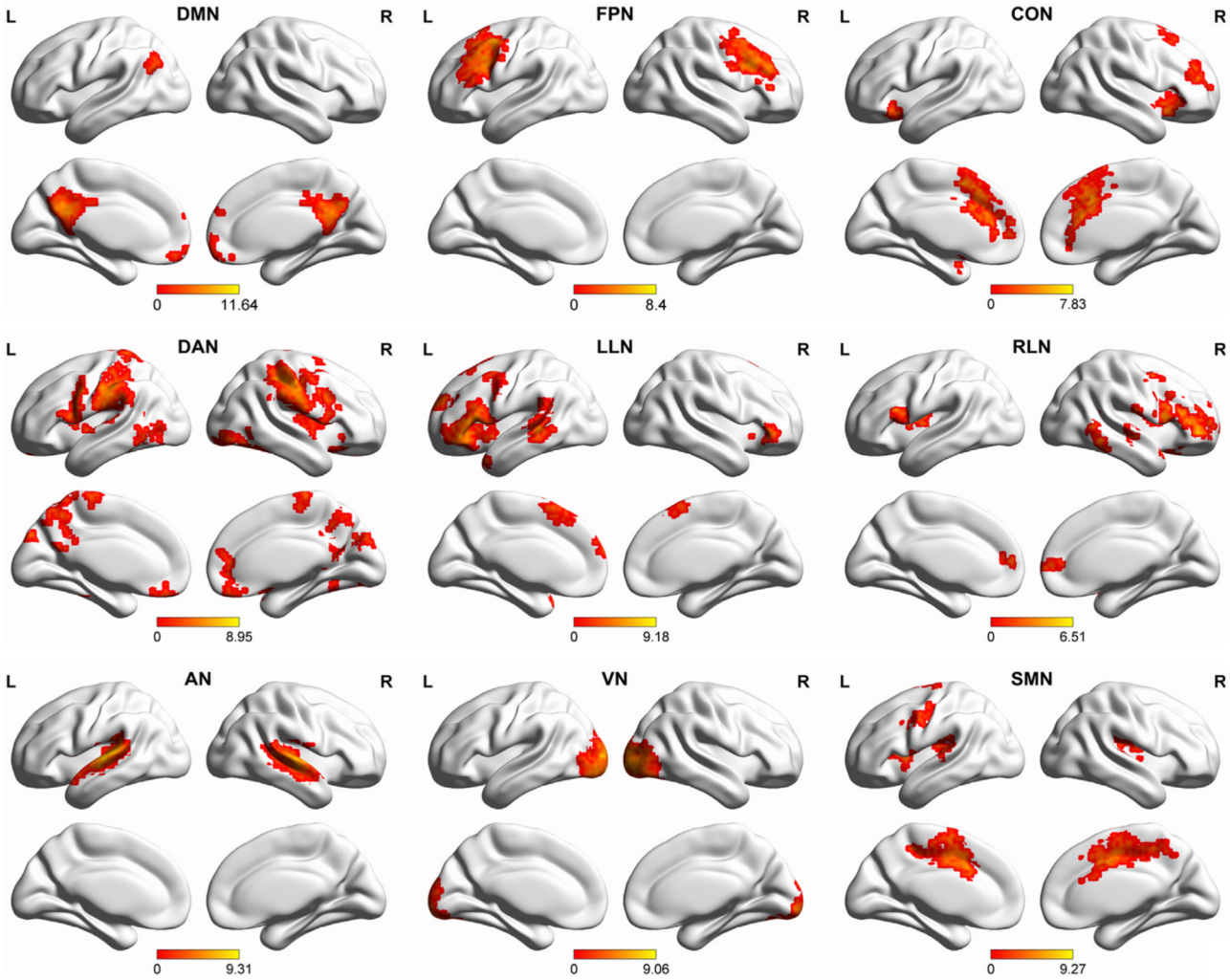

Fig. 5.

Fisher's Z-scores maps of each of the nine RSNs of interest ($p < .05$, corrected using AlphaSim test with cluster sizes > 56 voxels). Fisher's Z-scores were mapped on the cortical surface by using BrainNet Viewer (Xia et al., 2013). L: left; R: right.

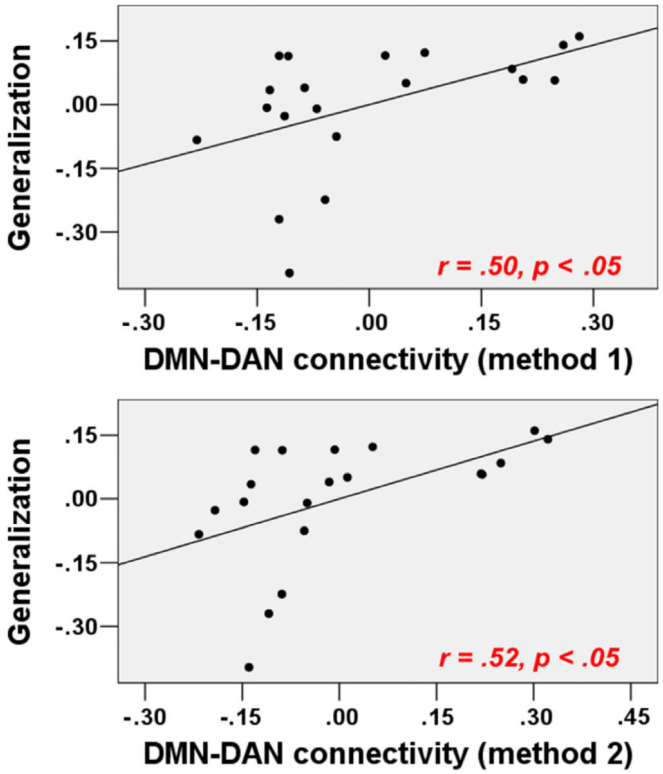

Fig. 6.

Correlations between DMN-DAN connectivity and Generalization scores after controlling for the effects of Tone ID and IQ (uncorrected $p < .05$).

Table 1

List of cortical anatomical regions and abbreviations used in the regional analysis.

Region	Abbreviation	Region	Abbreviation
Anterior cingulate gyrus	ACG	Superior temporal gyrus	STG
Angular gyrus	ANG	Temporal pole (superior)	TPOsup
Calcarine cortex	CAL	Temporal pole (middle)	TPOmid
Caudate	CAU	Orbitofrontal cortex (middle)	ORBmid
Hippocampus	HIP	Olfactory	OLF
Superior temporal gyrus	HG	Posterior cingulate gyrus	PCG
Inferior temporal gyrus	ITG	Parahippocampal gyrus	PHG
Inferior occipital gyrus	IOG	Precuneus	PCUN
Insular	INS	Supplementary motor area	SMA
Middle temporal gyrus	MTG	Superior frontal gyrus (dorsal)	SFGdor
Middle occipital gyrus	MOG	Superior frontal gyrus (medial)	SFGmed
Superior frontal gyrus	SFG	Superior occipital gyrus	SOG

Table 2

Correlations between Generalization scores and cognitive measures.

Measure	Age	Gender	IQ	AWM	SB	Tone ID
Generalization	.05	.17	.55*	.19	.27	.73**
Age		−.24	.02	−.04	.06	.07
Gender			.38	−.08	.11	.18
IQ				.42	−.03	.42
AWM					.44	.24
SB						.43

* $p < .05$

** $p < .001$. AWM: auditory working memory; SB: sound blending (measure of phonological awareness); Tone ID: tone identification pre-training.

Table 3

Clusters in which ALFF values were significantly correlated with Generalization scores.

Region (BA)	*r* (peak/cluster)	No. of voxels	Peak MNI coordinates		
			x	*y*	*z*
Areas in which ALFF values were positively correlated with Generalization scores					
LSTG/LHG(79/81)	.66/0.74	90	−51	−15	12
Areas in which ALFF values were negatively correlated with Generalization scores					
RITG (90)	−.79/−.81	92	60	−21	−21
ORBmid (25/16)	−.75/−.80	85	−3	54	−12
PCUN/PCG (66/67/33/34)	−.80/−.83	211	−12	−57	24
RSFGdor (4)	−.75/−.89	83	30	54	12
RACG/LSFGmed (32/23)	−.75/−.82	115	6	45	21
RANG/RMTG (66/86)	−.75/−.64	146	57	−54	21
LIPL/LANG (61/65)	−.85/−.48	115	−48	−51	39
RSFGmed (24)	−.80/−.82	183	12	33	55

L: left; R: right; STG: superior temporal gyrus; HG: Heschl gyrus; ITG: inferior temporal gyrus; ORBmid: orbitofrontal cortex (middle); PCUN: precuneus; PCG: posterior cingulate gyrus; SFGdor: superior frontal gyrus (dorsal); ACG: anterior cingulate gyrus; MTG: middle temporal gyrus; IPL: inferior parietal lobule; ANG: angular gyrus; SFGmed: superior frontal gyrus (medial).

Table 4

Correlations between nodal measures and Generalization scores.

Measures	Regions (labels in AAL_90/AAL_1024 atlas)			
AAL-90 [a]				
d_{nodal}	LSTG (81)[#]	LIOG (53)	LANG (65)[#]	LPCG (35)[#]
	.64 (.004)	.71 (.001)	–.69 (.002)	–.63 (.005)
E_{nodal}	LSTG (81)[#]			
	.72 (.001)			
N_{bc}	LMOG (51)			
	–.70 (.001)			
AAL-1024 [b]				
d_{nodal}	LSOG (270)	LSTG (947)[#]	LSTG (1009)[#]	LIOG (998)
	.69 (.002)	.64 (.004)	.64 (.004)	.65 (.004)
	LPCUN (234)[#]	LPHG (286)	RCAL (294)	LTPOmid (553)
	–.72 (.001)	–.77 (.0002)	.64 (.004)	–.68 (.002)
	RMFG (595)	RPHG (663)	RFFG (807)	RSFGmed (930)
	–.69 (.002)	–.64 (.004)	–.68 (.002)	–.69 (.002)
	LPHG (1013)			
	–.67 (.003)			
E_{nodal}	LSTG (146)[#]	LIOG (998)	LSTG (1009)[#]	RSFGdor (595)
	.67 (.002)	.66 (.003)	.66 (.003)	–.65(.004)
	LMFG (899)			
	–.66 (.003)			
N_{bc}	LMOG (905)			
	–.75 (.001)			

[a] The lower/upper critical correlation coefficients obtained by permutation tests for d_{nodal}, E_{nodal} and N_{bc} corresponded to –.73/0.72, –.69/0.71, and –.76/0.77, respectively.

[b] The lower/upper critical correlation coefficients obtained by permutation tests for d_{nodal}, E_{nodal}, and N_{bc} corresponded to –.77/0.77, –.78/0.78, and –.76/0.77, respectively. The p values (in parentheses) were not corrected for multiple comparisons. d_{nodal}: nodal degree; E_{nodal}: nodal efficiency; N_{bc}: nodal betweenness.

[#] in these regions, ALFF values were significantly correlated with Generalization scores.

Table 5

Correlations between inter-network interactions and Generalization scores.

	Inter-network correlations using method 1/method 2							
	DMN-LLN	**DMN-RLN**	**DMN-DAN**	**DMN-PFN**	**DMN-CON**	**DMN-AN**	**DMN-VN**	**DMN-SMN**
Generalization	.23/0.09	.17/0.31	.50[a]/0.52[a]	.14/0.13	.30/0.16	.25/0.33	.41/0.45	.09/0.10

[a] $p < .05$. The p values were not corrected for multiple comparisons.